BEAM PROFILE IMAGING BASED ON BACKWARD TRANSITION RADIATION IN THE EXTREME ULTRAVIOLET REGION*

L.G. Sukhikh†, S. Bajt, G. Kube, DESY, Hamburg, Germany,
Yu.A. Popov, A.P. Potylitsyn, Tomsk Polytechnic University, Tomsk, Russia,
W. Lauth, Institute for Nuclear Physics, Johannes Gutenberg University, Mainz, Germany

Abstract

The present report summarizes the results of a first transverse beam profile imaging experiment based on monochromatic backward emitted transition radiation in the extreme ultraviolet (EUV) region. In this test experiment beam spots are imaged using transition radiation in both EUV and optical regions. It is shown that EUV transition radiation is well suited for standard beam profile diagnostics.

INTRODUCTION

Optical Transition Radiation (OTR) is generated when a charged particle crosses the boundary between two media with different optical properties, and it is an important tool for beam diagnostics, mainly for transverse profile beam imaging, in modern linear accelerators. OTR in backward direction is generated directly at the screen boundary in an instantaneous process with a linear response and rather high light output. The radiation is emitted in direction of the specular reflection in a small lobe with an opening angle defined by the beam energy. Unfortunately, there are two physical limitations that make the method ineffective for reliable diagnostics in modern accelerators.

The experience from modern linac–based light sources showed that OTR diagnostics might fail even for high energetic electron beams because of coherent effects in the OTR emission process. It is well known that in the case when the radiation wavelength is longer than the bunch length, the radiation intensity scales quadratically with the bunch population. Despite that the electron bunch lengths in modern Free Electron Lasers (FELs) are significantly larger than optical wavelengths, some unstable micro structures, that radiate coherently, might appear in the bunch. In case of coherent OTR generation, an electron beam with Gaussian transverse profile is imaged as a donut structure. Coherent OTR was observed e.g. at the Linac Coherent Light Source LCLS in Stanford (USA) [1] and at FLASH at DESY in Hamburg (Germany) [2]. As consequence, for the new generation x-ray sources, such as the European X–FEL which is currently under construction in Hamburg [3], new reliable tools for transverse beam profile measurements are required.

The second physical limitation, that is an OTR point spread function (PSF), defines the minimum beam size that can be resolved using OTR. The PSF was investigated for the first time by M. Castellano and V.A. Verzilov [4] and later in more details by A.P Potylitsyn [5], D. Xiang and W.-H. Huang [6] and by G.Kube [7]. It was shown that the PSF has a double lobe structure defined by the observation wavelength and the acceptance of the optical system. The minimum beam size that can be measured using OTR with a wavelength of 400 nm and a reasonable optical system is about 1 μm.

In principle it is possible to overcome both limitations by decreasing the observation wavelength used for the beam imaging. The proposal to use backward transition radiation (BTR) in the Extreme Ultraviolet (EUV) region ($\lambda \simeq$ 20 nm) as a possible tool for transverse bunch profile diagnostics was published in Ref. [8]. In a previous publication the measurement of the EUV BTR angular distributions has been reported [9, 10]. In this paper we present the results of the first beam profile imaging experiments using BTR in the EUV region.

EXPERIMENTAL SETUP

The experiment was carried out at the 855 MeV electron beam of the Mainz Microtron MAMI (Institute for Nuclear Physics, Gutenberg University, Mainz, Germany). The quasi–continuous beam of the racetrack microtron (mean beam current 2.4 nA) was operated in macropulse mode with a pulse duration of 0.8 s in order to allow CCD frame readout in the gaps in between.

Figure 1 shows a scheme of the experimental setup. The BTR target was mounted onto a motorized stage which allowed rotation and linear motion along and across the beam axis. The electron beam interacted with the target, generating BTR in a wide spectral range. The short wavelength limit of the spectrum was defined by the reflection coefficients of the target material. The BTR was focused and monochromatized by a multilayer spherical mirror, the resulting beam image was recorded with a CCD detector. The distance from the target to the mirror was about 282 mm, the distance from the mirror to the CCD 2535 mm. A set of filters was mounted in front the CCD camera in order to selectively detect the optical or EUV part of the spectrum.

The BTR target consisted of a 50 nm thick molybdenum layer (surface roughness better than 0.5 nm), evaporated onto a 0.7 mm thick silicon substrate (dimensions 50 mm × 50 mm). The angle between electron beam and target normal amounted to 74° (grazing angle 16°).

The spherical multilayer Mo/Si mirror with 25.4 mm diameter and 250 mm focal distance used for BTR focussing

* This work was partly supported by the Russian Ministry for Science and Education within the program "Scientific and educational specialists of innovation Russia" under the contract No. П790 (24.05.2010).

† leonid.sukhikh@desy.de

ISBN 978-3-95450-115-1

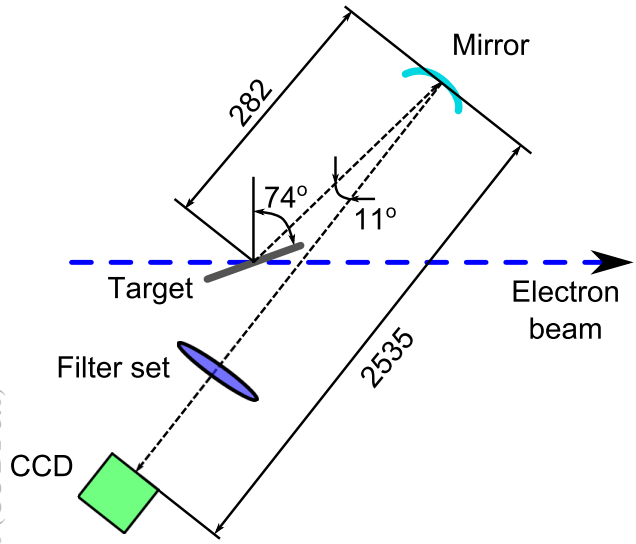

Figure 1: Experimental setup.

was designed and manufactured at DESY. At the central wavelength of 19.55 nm (64 eV) the peak mirror reflectivity was about 31% and the transmission width amounted to 2.6 nm (FWHM). The mirror normal was tilted with respect to the BTR emission direction by approx. 5.5°. However, such a tilt results in rather strong spherical aberration effects.

The beam images were recorded with a scientific grade CCD camera (ANDOR DO434-BN-932) with 1024×1024 pixels and a pixel size of $13 \times 13 \mu m^2$. Special feature of this in–vacuum CCD camera was a rather high sensitivity in the range from 1 eV up to 10 keV due to the back illuminated chip without coating. The CCD was cooled down to −20 °C in order to decrease dark current and CCD noise.

The filter set mounted onto a motorized holder was installed in front of the CCD. An optical bandpass filter (λ = 400 nm) was used to image the beam profile in the visible region, a 1.3 μm thick aluminum foil to block visible light and to image the beam only with EUV radiation. Filter and CCD characteristics are both shown in Fig. 2.

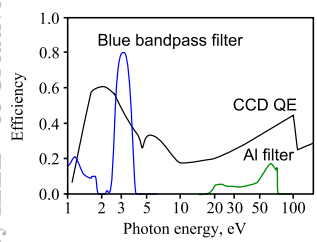

Figure 2: Transmission coefficients of the filters and CCD quantum efficiency.

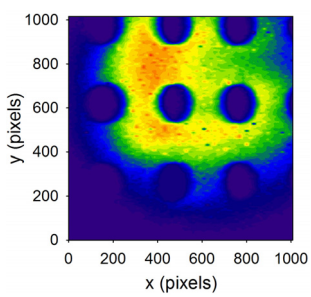

Figure 3: Calibration target image.

An optical grid target with a grid of dots (period 0.5 mm) was used to calibrate the optical system. In the beginning of the experiment it was installed instead of the BTR target and was illuminated by a blue LED. During the optical system adjustment the distance between target and mirror was changed in order to obtain the best focusing in horizontal and in vertical direction. The resulting image is shown in Fig. 3. Because of spherical aberrations, horizontal and vertical calibration coefficients were not identical and amounted to 1.69 μm and 1.43 μm per CCD pixel, respectively.

Both background and CCD noise were measured with the beam while the optical path was blocked by a 1 mm thick aluminum plate. The beam images obtained were averaged over 100 shots for the EUV region and over 20 shots for the optical region.

BEAM IMAGING IN THE EUV REGION

Figure 4 shows a beam image obtained in the optical region using the optical bandpass filter, Fig. 5 the image in the EUV region using the aluminum foil filter for the same electron beam parameters. The spots in Fig. 5 seem to be caused by a thin water layer condensed on the CCD surface. The radiation intensity is expressed in CCD counts per pixel, normalized to a single shot.

Comparing Fig. 4 with Fig. 5 one can see that the EUV radiation intensity is higher than the optical one. This might be surprising considering that the EUV radiation was substantially suppressed by the thick Al filter. However, this rather intense EUV BTR was observed previously [9, 10] and is one of the properties that makes using EUV BTR attractive.

Figure 6 shows a comparison of the horizontal and vertical projections of both beam images. One can clearly see that the measured beam sizes are larger in the case of optical radiation. The projections were fitted by Gaussian distributions with the following results for the (rms) widths: optical region $\sigma_x^{opt} = 51\,\mu$m, $\sigma_y^{opt} = 56\,\mu$m; EUV region $\sigma_x^{EUV} = 43\,\mu$m, $\sigma_y^{EUV} = 42.5\,\mu$m. This large discrepancy in beam size measurements using different spectral regions is currently not understood and most likely can not be explained just with better diffraction limited resolution of EUV radiation. In our opinion most likely explanation for the observed additional broadening of the optical beam image is due to aberrations in the optical system and a small mis-focusing.

SUMMARY AND OUTLOOK

The first electron beam imaging using EUV BTR is reported and compared with imaging in the visible region for the same electron beam parameters. Both methods resulted in the same beam shape and similar beam sizes. However, the beam sizes obtained during the EUV imaging were $15 - 25\%$ smaller than the ones obtained in the optical region, which might be explained by optical imperfections.

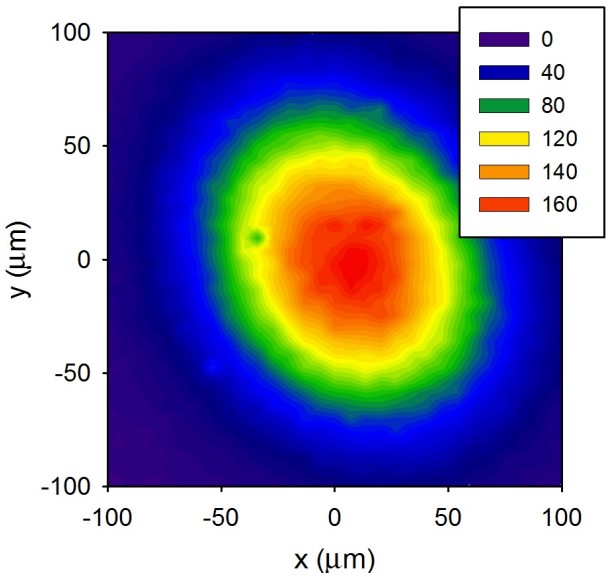

Figure 4: Beam image obtained in the optical region.

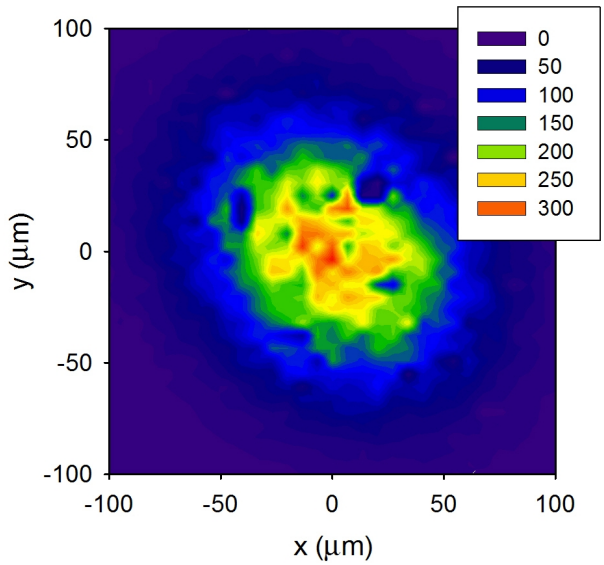

Figure 5: Beam image obtained in the EUV region.

The measured EUV intensity was almost twice as high as the visible radiation. The results of this first test experiment show that BTR in the EUV region is a promising candidate for an improvement of standard optical transverse beam diagnostics with better resolution and void of coherent effects. As one of the next steps we plan to demonstrate that EUV BTR is an efficient method to overcome the problem of coherent optical radiation, and to improve the resolution in view of sub–micron beam size imaging.

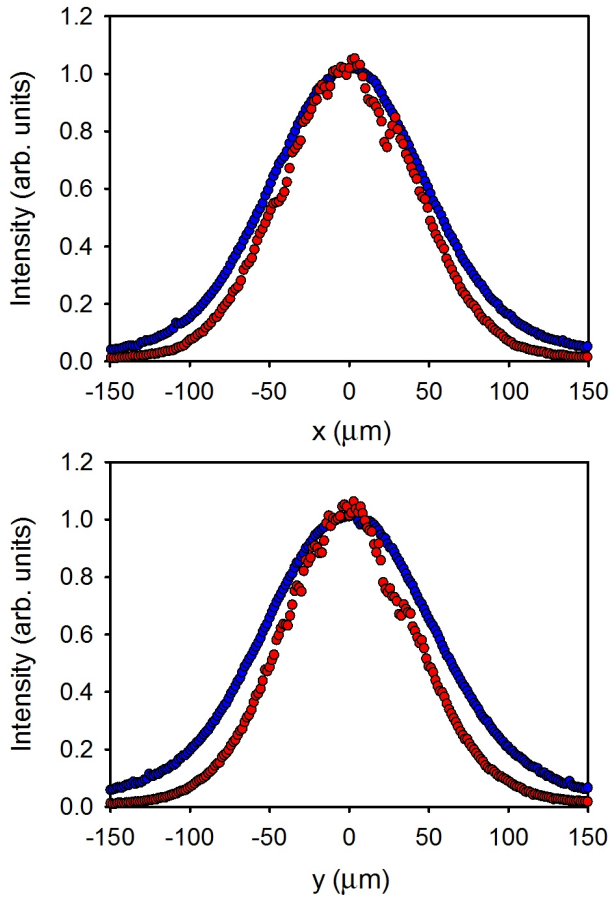

Figure 6: Horizontal and vertical projections of beam images obtained in both optical (blue dots) and EUV (red dots) regions. For better comparison the projections are normalized to the peak value.

REFERENCES

[1] H. Loos et al., Proc. FEL '08, THBAU01, Gyeongju, South Korea, p. 485 (2008).

[2] S. Wesch, C. Behrens, B. Schmidt, P. Schmüser, Proc. FEL '09, WEPC50, Liverpool, UK, p. 619 (2009).

[3] XFEL Technical Design Report, DESY 2006-097, http://xfel.desy.de

[4] M. Castellano and V. A. Verzilov, Phys. Rev. Spec. Top. Accel. Beams 1 (1998) 062801.

[5] A.P. Potylitsyn, in *Advanced Radiation Sources and Applications* ed. by H. Wiedemann (2006) 149.

[6] D. Xiang, W.-H. Huang, Nucl. Instr. Meth. Phys. Res. A 570 (2007) 357.

[7] G. Kube, Imaging with Optical Transition Radiation, Transverse Beam Diagnostics for the XFEL, TESLA-FEL 2008-01 (2008).

[8] L.G. Sukhikh, S.Yu. Gogolev, and A.P. Potylitsyn , Nucl. Instrum. Methods Phys. Res., Sect. A 623(1) (2010) 567.

[9] L.G. Sukhikh, D. Krambrich, G. Kube, W. Lauth, Yu.A. Popov, and A.P. Potylitsyn, SPIE Optics and Optoelectronics proceedings 8076, Prague, Czech Republic, p. 80760G-1 (2011).

[10] L.G. Sukhikh, D. Krambrich, G. Kube, W. Lauth, Yu.A. Popov, and A.P. Potylitsyn, Proc. DIPAC '11, WEOA02, Hamburg, Germany, p. 544 (2011).

ISBN 978-3-95450-115-1